



SEJERVEN  
MORRILL  
MACPHERSON LLP

7-31-00

A

Docket No.: M-8821 US

July 27, 2000

Box Patent Application  
Commissioner For Patents  
Washington, D. C. 20231

Enclosed herewith for filing is a patent application, as follows:

Inventors: Roman Sobolewski; Grigory N. Gol'tsman; Alexey D. Semenov; Oleg V. Okunev; Kenneth R. Wilsher; Steven A. Kasapi

Title: Superconducting Single Photon Detector

X Return Receipt Postcard  
X This Transmittal Letter (in duplicate)  
21 Pages Specification (not including claims)  
3 Pages Claims  
1 Page Abstract  
16 Sheets of Drawings (FIGs. 1A, 1B, 1C, 2A, 2B, 2C, 2D, 3A, 3B, 3C, 3D, 3E, 3F, 3G, 3H, 3I, 3J, 3K, 3L, 4A, 4B, 4C, 5, 6A, 6B, 7, 8A, 8B, 8C)  
3 Pages Declaration For Patent Application and Power of Attorney (unsigned)  
1 Pages Recordation Form Cover Sheet (in duplicate)  
5 Pages Assignment (unsigned)

**CLAIMS AS FILED**

For	Number <u>Filed</u>		Number <u>Extra</u>		Rate		Basic Fee
Total Claims	15	-20 =	0	x	\$18.00	=	\$ 0.00
Independent Claims	2	-3 =	0	x	\$78.00	=	\$ 0.00
<input type="checkbox"/> Fee of	for the first filing of one or more multiple dependent claims per application						\$
<input type="checkbox"/> Fee for Request for Extension of Time							\$

Please make the following charges to Deposit Account 19-2386:

- ☒ Total fee for filing the patent application in the amount of \$ 690.00
- ☒ The Commissioner is hereby authorized to charge any additional fees which may be required, or credit any overpayment to Deposit Account 19-2386.

EXPRESS MAIL LABEL NO:  
EL 276257470 US

Respectfully submitted,

*Patrick D. Benedicto*

Patrick D. Benedicto  
Attorney for Applicants  
Reg. No. 40,909



## SUPERCONDUCTING SINGLE PHOTON DETECTOR

Roman Sobolewski  
Grigory N. Gol'tsman  
Alexey D. Semenov  
Oleg V. Okunev  
Kenneth R. Wilsher  
Steven A. Kasapi

### 10 BACKGROUND OF THE INVENTION

#### Field of the Invention

The present disclosure generally relates to  
15 photodetectors and more particularly to single photon  
detectors.

#### Description of the Related Art

20 A photodetector is a device that provides an  
electrical voltage or electrical current output signal  
when light is incident thereon. There are two basic  
types of photodetectors: linear detectors and quantum  
detectors. Linear detectors provide an output signal  
25 that is a linear function of the incident light  
intensity or average optical power. Quantum detectors  
provide an output signal upon detection of photons of  
the incident light.

30 A single-photon detector is a quantum detector  
that can detect one incident photon at a time.  
Commercially available single photon detectors detect  
photons in the visible and shorter wavelength optical  
regions of the electromagnetic spectrum. These  
35 commercially available detectors include silicon  
avalanche photodiodes (Si APDs), such as part number

C30954 from EG&G Optoelectronics. A typical Si APD has a responsivity of 70 A/W (amps/watt) for photons with wavelengths of 900nm, which drops to 36 A/W for photons with wavelengths of 1064nm. Currently available Si APDs  
5 are not sensitive enough to detect photons with wavelengths longer than 1100nm.

Characteristics of hot-electron photodetectors that are fabricated from superconducting NbN (niobium  
10 nitride) films are discussed in K.S. Il'in, I.I. Milostnaya, A.A. Verevkin, G.N. Gol'tsman, E.M. Gershenzon, and Roman Sobolewski, "Ultimate Quantum Efficiency Of A Superconducting Hot-Electron Photodetector," Applied Physics Letters Vol. 73, No. 26  
15 (December 18, 1998), pages 3938-3940 and in K.S. Il'in, M. Lindgren, M. Currie, A.D. Semenov, G.N. Gol'tsman, Roman Sobolewski, S.I. Chereduichenko, and E.M. Gershenzon, "Picosecond Hot-Electron Energy Relaxation in NbN Superconducting Photodetectors," Applied Physics  
20 Letters Vol. 76, No. 19 (May 8, 2000), pages 2752-2754. Both publications are incorporated herein by reference. Some of the authors of the above mentioned articles are also inventors of this disclosure. While the first  
25 article suggests that "NbN HEPs should be able to detect single quanta of the far-infrared radiation and successfully compete as single-photon detectors with SIS-tunnel devices" (Applied Physics Letters, Vol. 73, No. 26 at p. 3940), there is no further relevant  
30 disclosure. The second article discusses the intrinsic response times of the hot-electron effect in NbN's, which applies to both linear and quantum NbN photodetectors.

### SUMMARY

The present disclosure addresses the above mentioned limitation of prior art photodetectors by providing a single-photon, time-resolving detector with good quantum efficiency for photons in the wavelengths from the visible to the far infrared spectral region.

In one embodiment, the single-photon detector includes a strip of superconducting material. The superconductor is biased with electrical current that is near the superconductor's critical current. The superconductor provides a discernible output pulse signal upon absorption of a single incident photon. In one embodiment, the superconductor is a narrow strip of NbN film. In another embodiment, the superconductor has a meandering shape to increase its surface area and thus also the probability of absorbing a photon from a light source.

The present single-photon detector can be used in a variety of applications including free-space and satellite communications, quantum communications, quantum cryptography, weak luminescence, and semiconductor device testing.

### BRIEF DESCRIPTION OF THE DRAWINGS

FIG. 1A shows a block diagram of a photon counter using the present superconducting single-photon detector (SSPD).

FIG. 1B shows a plan view of an SSPD.

FIG. 1C shows a plan view a of an SSPD having a meandering shape.

FIGS. 2A-2D graphically illustrate the physical process which the inventors believe gives rise to the

voltage that develops across an SSPD upon absorption of a single photon.

FIGs. 3A-3L show cross-sectional views of an SSPD being fabricated.

5        FIG. 4A shows a block diagram of an apparatus including the present SSPD.

FIG. 4B shows further details of the biasing arrangement for the SSPD shown in FIG. 4A.

10       FIG. 4C shows a typical current-voltage (I-V) plot for an SSPD at 4.2 Kelvin.

FIG. 5 shows plots of the probability of detecting an output pulse from an SSPD as a function of either incident light energy per pulse or, equivalently, the number of photons per device, per pulse using the  
15       apparatus shown in FIG. 4A.

FIGs. 6A and 6B show waveforms of a typical output signal of the SSPD used in the apparatus shown in FIG. 4A.

20       FIG. 7 shows oscilloscope traces of output signals of the SSPD used in the apparatus shown in FIG. 4A.

FIGs. 8A-8C show schematic diagrams of various arrangements for coupling light to an SSPD.

The use of the same reference symbol in different  
25       figures indicates the same or identical elements. Further, the figures in this disclosure are schematic representations and not drawn to scale.

#### DETAILED DESCRIPTION

30

FIG. 1A shows a block diagram of a photon counter  
10       including a superconducting single-photon detector (SSPD) in accordance with an embodiment of the invention. Referring to FIG. 1A, an SSPD 12 detects  
35       photons 16 emitted by a light source 11, which includes suitable optics (not shown). It is to be understood

that light source 11 is not necessarily a part of photon counter 10 and is, for example, a transistor which emits photons when switching. Upon absorption of an incident photon, SSPD 12 in response generates an electrical output pulse signal that is amplified by associated amplifier 13. Each output pulse signal is recorded and counted by data acquisition system (DAQ) 14 (e.g., a computer equipped with appropriate interface circuitry and software).

10

In one embodiment, SSPD 12 is a narrow, thin strip of a superconducting material that is electrically biased to provide an output pulse signal upon absorption of a single incident photon. As shown in the plan view of FIG. 1B, SSPD 12, in this example, is a narrow strip of NbN (niobium nitride) film having a width D1 of about 200nm, a length D2 of about 1 $\mu$ m, and a thickness of about 5nm. A direct current (DC) bias source (not shown) provides biasing current to SSPD 12 through gold contact pads 42. SSPD 12 and contact pads 42 are conventionally disposed on a substrate; suitable substrates include sapphire and quartz for infrared and visible light applications. Silicon can also be used as a substrate, e.g. for infrared applications. SSPD 12 typically, but not necessarily, faces light source 11. In the absence of incident photons and while SSPD 12 is conventionally cooled to a superconducting state, the voltage across SSPD 12 is zero because SSPD 12 is a superconductor and hence has zero resistance when in the superconducting state. A photon incident on SSPD 12 switches it into the resistive state, thereby developing a voltage drop across SSPD 12 detected by DAQ 14.

As is well known, a superconductor, such as SSPD 12, remains in a superconducting state only while the

amount of current being carried by the superconductor, the temperature of the superconductor, and the external magnetic field surrounding the superconductor are maintained below certain values referred to as critical values. The critical values (i.e., critical current, critical temperature, and critical magnetic field) are characteristic of the superconducting material and its dimensions. To maintain SSPD 12 in the superconducting state in the absence of incident photons, SSPD 12 is maintained at a temperature below 10 Kelvin (the approximate critical temperature of a thin NbN film) such as 4.2 Kelvin and exposed to ambient Earth magnetic field as is conventional with superconductors. The biasing current through SSPD 12 is set just below the critical current to increase its sensitivity, thereby allowing single-photon detection. The critical current of SSPD 12 is experimentally determined by maintaining SSPD 12 well below its critical temperature and critical magnetic field and then increasing the amount of current flown through SSPD 12 until it transitions from a superconducting state (zero resistance) to a resistive state (some resistance).

FIGS. 2A-2D graphically illustrate the physical process which the inventors believe gives rise to the voltage pulse that develops across SSPD 12 upon absorption of a single photon. However, understanding of this is not necessary for making or using the SSPD. The dashed arrows in FIGS. 2A-2D schematically represent the flow of the biasing current through SSPD 12. Referring to FIG. 2A, a photon incident on SSPD 12 creates a hot spot 21, a region where the temperature of electrons is much higher than SSPD 12's ambient temperature. The diameter of hot spot 21 directly depends on the energy of the incident photon. Within a few picoseconds, hot spot 21 diffuses further across

SSPD 12 and becomes a larger hot spot 22 (FIG. 2B). Hot spot 22 defines a region in SSPD 12 that is no longer superconducting. Because hot spot 22 is a resistive region, the biasing current is forced to flow around hot spot 22 and into regions between hot spot 22 and the edges of SSPD 12 that are still superconducting. This increases the current density in the still superconducting regions above the critical current density, thereby destroying superconductivity and creating resistive regions 24 (also known as phase slip centers) (FIG. 2C). Thus, a resistive region 25 (FIG. 2D) is formed across the entire width of SSPD 12. Biasing current flowing through resistive region 25 develops a voltage signal across SSPD 12.

Following the formation of hot spot (i.e., resistive) regions is the cooling process associated with the diffusion of electrons out of the hot spot regions and simultaneous reduction of the electrons' temperature via the electron-phonon energy relaxation mechanism. The cooling process takes a few tens of picoseconds and results in the automatic disappearance of the hot spot (and resistive region 25) and reestablishment of a superconducting path across SSPD 12. The hot spot formation and the healing processes result in an output voltage signal having a pulse shape with an intrinsic width of approximately 30ps. The width of the voltage pulse is determined by the specifics of the superconducting material and the energy of the incident photon. Because the output voltage pulse has a duration of only tens of picoseconds, SSPD 12 (and other SSPDs in accordance with this disclosure) can time resolve incident photon energy, and can distinguish photons arriving at a very high rate (e.g., above  $10^9$  photons per second).



Referring back to FIG. 1B, dimension D1 of SSPD 12 is, in one embodiment, about 200nm. If dimension D1 is significantly wider than 200nm, a detectable resistive region 25 (FIG. 2D) may not be formed as the biasing current may remain superconducting at all times and be able to flow around the resulting hot spot without exceeding the current density around the hot spot. Dimension D1 can be increased for detection of very high energy (e.g., ultraviolet) photons. For detecting red to short-infrared photons, a dimension D1 of 200nm is suitable for an NbN SSPD. The length of the narrow section, dimension D2, is 1 $\mu$ m in one embodiment. The length of the narrow section does not affect the physical process that gives rise to the output voltage pulse but does change the surface area and hence the overall quantum efficiency of SSPD 12. The thickness of the narrow section is about 5nm in one embodiment. The thickness of an SSPD directly affects the hot electron thermalization and relaxation processes, which are responsible for the healing of hot spots. Of course, the dimensions and critical values provided here are specific to the disclosed examples (which are designed to detect red and short-infrared photons) and can be varied depending on the energy levels of the photons of interest and the superconducting material used. For example, the dimensions of SSPD 12 can be modified to detect photons having wavelengths in the ultraviolet, visible, or far infrared spectral region.

In general, any thin and narrow strip of superconducting material can be used as an SSPD in accordance with this disclosure. Other metallic superconductors (so-called low-temperature superconductors), such as Nb (niobium), Pb (lead), or Sn (tin) can be fabricated with somewhat wider D1 dimension for detecting red and short-infrared photons.

However, these other metallic superconductors are not as time resolving as is NbN because of their significantly longer output voltage response (in nanosecond to even microsecond range) which is due to their slow hot electron relaxation process. Recently discovered high-temperature superconductors, such Y-Ba-Cu-O (yttrium-barium-copper oxide compound), are predicted to require a D1 dimension on the order of about 10nm to 100nm and have a response time on the order of about 1ps.

FIG. 1C shows a plan view of a superconducting single photon detector 101 (SSPD 101) of the same type as SSPD 12. SSPD 101 has a meandering shape to maximize its top surface area and thereby increase its probability of receiving an incident photon from a light source. In one example, SSPD 101 is a continuous NbN film having a width D5 of about  $0.2\mu\text{m}$ , a device length D6 of about  $3\mu\text{m}$ , and a thickness of about 5nm. Other meandering shapes (e.g., zigzag shape) can also be used.

FIGS. 3A-3L show cross-sectional views of a superconducting single photon detector, such as SSPD 12, being fabricated in accordance with one embodiment. Steps that are well known and not necessary to the understanding of the fabrication process have been omitted. Further, while specific fabrication process parameters are provided, other embodiments are not so limited because one of ordinary skill in the art can use other fabrication processes to make an SSPD. Referring to FIG. 3A, a 5nm thick NbN film 32 is deposited on a substrate 31 by reactive magnetron sputtering. The reactive magnetron sputtering process is performed using an LH Z-400 sputtering system of the

type supplied by Leybold-Herauss of Germany with the following parameters:

- residual pressure is  $1.3 \times 10^{-6}$  mbar;
- substrate temperature is  $900^{\circ}\text{C}$ ;
- 5 partial  $\text{N}_2$  pressure is  $1.3 \times 10^{-6}$  mbar;
- partial Ar pressure is  $1.3 \times 10^{-3}$  mbar;
- discharge voltage is 260V;
- discharge current is 300mA.

- Substrate 31 is, for example, a  $350\mu\text{m}$  thick sapphire
- 10 substrate that is polished on the active side. Other substrates can also be used such as a  $125\mu\text{m}$  thick Z-cut single crystal quartz polished on both sides. Any high-quality dielectric material that has low microwave loss and good cryogenic properties can be used as a
- 15 substrate.

- FIGS. 3B-3D illustrate the formation of alignment structures on NbN 32 for subsequent photolithography and electron beam lithography steps. In FIG. 3B, a
- 20  $1.0\text{-}1.5\mu\text{m}$  thick photoresist mask 33 is formed and patterned on NbN 32 by conventional photolithography using the following parameters:

- photoresist material is AZ 1512;
- spinning at 3000-5000 rps;
- 25 baking at  $90^{\circ}\text{C}$ , 30 minutes.

- A KARL SUSS MA-56 aligner is used to align photoresist mask 33 over NbN 32. Over the resulting structure, a  $100\text{nm}$  thick gold layer 35 is formed on top of a  $5\text{nm}$  thick titanium layer 34 using a double layer
- 30 metallization process (FIG. 3C). Gold layer 35 and titanium layer 34 are formed by vacuum evaporation at room temperature and at a residual pressure of  $1.5 \times 10^{-5}$  Torr. Photoresist mask 33 is lifted off by immersing the structure in warm acetone for about 3 minutes or
- 35 longer, leaving alignment structures consisting of gold layer 35 and titanium layer 34 (FIG. 3D).

FIGS. 3E-3G illustrate the formation of internal contact pads on NbN 32. In FIG. 3E, a 400nm thick electron resist mask 36 is formed and patterned on NbN 32 by conventional electron beam lithography using the following parameters:

- electron resist material is PMMA 950, 475;
- spinning at 3000 rpm;
- baking at 130°C, 10-30 minutes;
- 10 electron beam exposure current is 30pA;
- electron beam exposure voltage is 25kV.

The length of the middle section of electron resist mask 36, shown in FIGS. 3E and 3G as dimension D2 (also, see FIG. 1B), can be varied from about 0.15μm to 15 10μm to change the effective length of the SSPD in one embodiment. Electron resist mask 36 is cleaned in an oxygen plasma using the following parameters:

- O<sub>2</sub> pressure is 10<sup>-2</sup> Torr;
- residual pressure is 10<sup>-5</sup> Torr;
- 20 discharge current of 10 mA;
- process time of 15 seconds.

A 400nm thick gold layer 37 is then formed on top of a 3nm thick chromium layer 38 using a double layer metallization process (FIG. 3F). Gold layer 37 and 25 chromium layer 38 are formed by vacuum evaporation using an LH-960 e-beam evaporation system from Leybold-Herauss of Germany at room temperature and at a residual pressure of 2x10<sup>-6</sup> Torr. Electron resist mask 36 is then lifted off, leaving internal contact pads 30 consisting of gold layer 37 and chromium layer 38 (FIG. 3G).

FIGS. 3H-3J illustrate the formation of a silicon dioxide mask (SiO<sub>2</sub>), a "hard" mask for later ion milling 35 processing steps. In FIG. 3H, electron resist mask 39 is formed on NbN 32 using a process similar to that

used to form electron resist mask 36 discussed above.  
A  $\text{SiO}_2$  layer 41 is then vacuum evaporated on the  
resulting structure as shown in FIG. 3I. Electron  
resist mask 39 is lifted off, leaving an  $\text{SiO}_2$  mask  
5 consisting of  $\text{SiO}_2$  layer 41 (FIG. 3J). The  $\text{SiO}_2$  mask,  
which is transparent to the photons, defines the width  
of the SSPD.

External contact pads, consisting of 200nm thick  
10 gold layer 42 on top of 7-10nm thick titanium layer 43,  
for coupling NbN 32 to external equipment such as a  
bias source are formed as shown in FIG. 3K. The  
external contact pads are formed using a process  
similar to that used to form gold layer 37 and chromium  
15 layer 38. Portions of NbN 32 between the external  
contact pads and the alignment structures are then  
removed by argon ion milling, defining the SSPD device  
(FIG. 3L).

FIG. 4A shows a block diagram of a pulse counter  
20 60 including an SSPD 12. In pulse counter 60, SSPD 12  
is a 200nm wide,  $1\mu\text{m}$  long, and 5nm thick NbN film.  
Light source 11 outputs light pulses 16 to a beam  
splitter 62, which splits the light for input to an  
25 attenuator 63 and a photodetector 64. In pulse counter  
60, light source 11 is a laser that generates short  
light pulses at a repetition rate of about 76 MHz when  
it is a modelocked IR laser from Coherent Laser Group  
(MIRA laser) or about 82 MHz when it is a modelocked  
30 laser from Spectra-Physics (Tsunami laser). Light  
source 11 can also be a GaAs semiconductor laser  
modulated from 1Hz to 3kHz. The wavelength of the  
photons from light source 11 is approximately 810nm in  
this example. In other experiments, single photon  
35 detection was also achieved with photons having  
wavelengths of 500nm to 2100nm. Attenuator 63 is a

series of absorbing filters used to reduce the number of photons incident on SSPD 12 to an average of less than one photon per pulse. For example, absorbing filters can be added to or removed from attenuator 63 so that the probability of having a photon in each pulse is 0.01, resulting in an average of one photon every 100 pulses.

Photons passing through attenuator 63 are focused onto SSPD 12 using conventional focusing lens 65. A direct current (DC) bias source 67 provides biasing current to SSPD 12 through a wide-band "cold" bias-T 66 (also shown in FIG. 4B). The output signal of SSPD 12 is coupled to a "cold" amplifier 68, through bias-T 66, for amplification prior to being transmitted outside a cryostat 69. Cryostat 69 is a conventional liquid helium cryostat that maintains SSPD 12 at a temperature below its critical temperature. Cold amplifier 68, a conventional cryogenic power amplifier, has a thermal equivalent noise ( $T_{noise}$ ) of about 5 Kelvin, frequency range of 1-2 GHz, and gain ( $K_p$ ) of 30dB. Bias-T 66, cold amplifier 68, and SSPD 12 are conventionally housed within cryostat 69. The output signal of cold amplifier 68 is further amplified by a power amplifier 70 to boost the output signal of SSPD 12 to a level detectable by a single shot oscilloscope 71. Power amplifier 70 has a specified peak output power of about 0.2W, frequency range of 0.9-2.1 GHz, and gain ( $K_p$ ) of 32dB.

A conventional photodetector 64 detects the split-off light pulses from beam splitter 62 and provides an output signal that triggers oscilloscope 71 to acquire the signal from power amplifier 70. A CCD video camera 72 takes a picture of the screen of oscilloscope 71, which is then downloaded to a computer 73 with video

capture hardware for analysis. The data acquisition elements which include oscilloscope 71, CCD video camera 72, and computer 73 are, like the other depicted elements, exemplary.

5

FIG. 4B shows further details of the electrical biasing arrangement for SSPD 12. As shown in FIG. 4B, 50-Ohm transmission lines 402 (i.e., transmission lines 402A, 402B, 402C, and 402D) are used to couple SSPD 12 to bias-T 66, DC bias source 67, and cold amplifier 68. The coupling between SSPD 12 and transmission line 402A is through a conventional high-bandwidth connection 401, which is part of the SSPD 12 housing. Bias-T 66 has a DC port and an AC port which are schematically depicted in FIG. 4B as inductor "L" and capacitor "C". The inductor and capacitor of bias-T 66 are preferably not dependent on temperature. One can also measure the performance of a particular bias-T 66 at cryogenic temperatures and determine the appropriate component values based on how the component values shift with temperature. Appropriate component values in this example are  $0.2\mu\text{H}$  or greater for inductor "L" and 1000 pF or greater for capacitor "C" at a temperature of about 4 Kelvin. The pulsed voltage output signal from SSPD 12 is applied to the AC port of bias-T 66 and amplified by cold amplifier 68 before being transmitted out of cryostat 69 via transmission line 402C. Bias current from DC bias source 67 is provided to SSPD 12 through the DC port of bias-T 66. DC bias source 67 has a variable DC current source 403 for providing bias current, a current meter 406 for reading the supplied bias current, and a voltage meter 405 for reading the voltage across SSPD 12. DC bias source 67 also includes an adjustable voltage limit 407 to limit the voltage across SSPD 12 when it switches to the resistive state. A typical setting for voltage limit

407 is about 3mV to 5mV. The critical current of SSPD 12 is determined by maintaining SSPD 12 well below its critical temperature using cryostat 69 (note that the ambient Earth magnetic field is well below the critical magnetic field of SSPD 12). DC current source 403 is then adjusted until SSPD 12 transitions from the superconducting state to the resistive state. The bias current, read using current meter 406, which transitions SSPD 12 into the resistive state is the critical current. SSPD 12 is normally operated with a bias current that is below the critical current. A typical range of biasing current for SSPD 12 is 40-50 $\mu$ A. Preferably, the biasing current is set as close to the critical current as possible without falsely transitioning SSPD 12 into the resistive state in the absence of an incident photon.

FIG. 4C shows a typical current-voltage plot for SSPD 12 at 4.2 Kelvin. In FIG. 4C, the vertical axis indicates the DC bias current through SSPD 12 (in  $\mu$ A) as measured by current meter 406 while the horizontal axis indicates the DC voltage drop across SSPD 12 as measured by voltage meter 405 (FIG. 4B). As indicated in FIG. 4C, the critical current of SSPD 12 is approximately 45 $\mu$ A. As long as the bias current is below the critical current, SSPD 12 remains in the superconducting state represented by the vertical trace beginning at 0mV. Although the biasing current through SSPD 12 is 40 $\mu$ A, the voltage across SSPD 12 remains at 0mV while SSPD 12 is in the superconducting state (because SSPD 12 is a superconductor and hence has zero resistance in the superconducting state). Thus, SSPD 12 remains on operating point "A" under normal conditions. When SSPD 12 absorbs a photon, SSPD 12 can become resistive thereby causing the current through it to drop and the voltage across it to rise. This moves



the operating point of SSPD 12 from point "A" to a point "B" on a dashed trace labeled "Meta Stable Region" in FIG. 4C. Note that points "A" and "B" are connected by a solid 50-Ohm load trace, which reflects the impedance of the 50-Ohm transmission line presented to SSPD 12. The separation point between the Meta Stable Region and the Normal Resistance Region is the voltage level corresponding to the critical current multiplied by the 50-Ohm load resistance, which comes out to 2.25mV (i.e.,  $45\mu\text{A} \times 50\Omega = 2.25\text{mV}$ ) in the example of FIG. 4C. For a short time (tens of picoseconds) after absorption of the photon, the operating point of SSPD 12 remains on point "B". Thereafter, the operating point of SSPD 12 returns to point "A". If the current through SSPD 12 is increased enough, to slightly above  $45\mu\text{A}$  in the example shown in FIG. 4C, the bias current will exceed the critical current thereby moving the operating point of SSPD 12 to point "C" on the trace labeled "Normal Resistance Region". While at operating point "C", photon detection is not possible because SSPD 12 will remain in the resistive state until its bias current is lowered below the critical current. Note that the voltage across SSPD 12 on point "C" is limited by the setting of voltage limit 407, which is 3mV in this example.

As will be demonstrated below, single photon detection requires a linear dependence on the number of absorbed photons. For a mean number of  $m$  photons absorbed per laser pulse, the probability of absorbing  $n$  photons from a given pulse is

$$P(n) = \frac{e^{-m} (m)^n}{n!}$$

When  $m \ll 1$ ,

$$P(n) = \frac{m^n}{n!}$$

For the apparatus shown in FIG. 4A,  $m \ll 1$  can be achieved by adjusting attenuator 63 such that the

- 5 number of photons incident on SSPD 12 is reduced to an average of much less than one per laser pulse. From the foregoing, the probability of absorbing 1 photon per pulse is

$$P(1) = m$$

- 10 The probability of absorbing 2 photons per pulse is

$$P(2) = \frac{m^2}{2}$$

(Of course,  $P(2)$  is the probability of absorbing two photons on the same spot on the superconducting film at the same time; otherwise, the two photons would count as two single photons). The probability of absorbing 3

- 15 photons per pulse is

$$P(3) = \frac{m^3}{6}$$

Thus, for  $m \ll 1$ , the probability of detecting one photon per pulse is proportional to  $m$ , the probability of detecting two photons is proportional to  $m^2$ , the probability of detecting 3 photons is proportional to  $m^3$ , and so on.

- FIG. 5 shows plots of the probability of SSPD 12 producing an output voltage pulse in one experiment. In FIG. 5, the vertical axis indicates the probability of SSPD 12 detecting a photon in a single light pulse, based on the number of light pulses detected by pulse counter 60 over a long period of time. The lower
- 25
- 30 horizontal axis indicates the average energy (in femtojoules) of each light pulse focused on SSPD 12

while the upper horizontal axis indicates the computed corresponding number of incident photons per light pulse, per  $0.2 \times 1 \mu\text{m}^2$ , which is the area of SSPD 12 in the experiment. The critical current,  $I_c$ , was  
5 experimentally determined to be around  $45 \mu\text{A}$ .

Trace 501 corresponds to an SSPD 12 that was biased to  $0.95 I_c$  (i.e., 95% of the critical current). Trace 501 shows the linear dependence of detection  
10 probability to the average number of photons per pulse, indicating single photon detection. Trace 502 corresponds to an SSPD 12 that was biased to  $0.9 I_c$ . Trace 502 shows a quadratic dependence of detection  
15 probability to the average number of photons per pulse, indicating two photon detection. Further reducing the bias current of SSPD 12 to  $0.7 I_c$  results in trace 503. Trace 503 shows a cubic dependence of detection  
20 probability to the number of photons per pulse, indicating three photon detection. From the foregoing, setting the bias current of SSPD 12 near its critical current allows single photon detection.

FIG. 6A shows a waveform of a typical output signal of SSPD 12. Pulse 81, which corresponds to a  
25 detected incident photon, is readily distinguishable from background noise. As shown in the magnified view of FIG. 6B, pulse 81 has full width half maximum (FWHM) of about 100ps. The bandwidth of pulse 81 was limited by the bandwidth of the data acquisition equipment  
30 used, not by SSPD 12. In FIGs. 6A and 6B, the vertical axis is in an arbitrary unit of voltage while the horizontal axis is in nanoseconds. An SSPD in accordance with this disclosure simplifies the detection process by providing an output voltage pulse  
35 that is readily read using conventional data acquisition techniques.

Spectroscopic information about the energy of the detected photon can also be obtained by analyzing the shape of the output signal of an SSPD. A hot electron is created when a photon is absorbed by the SSPD and breaks a so-called Cooper pair. The hot electron collides with other Cooper pairs in the SSPD, thereby breaking the Cooper pairs and creating more hot electrons. Because the number of broken Cooper pairs is proportional to the energy of the incident photon, and the shape of the output voltage pulse depends on the number of hot electrons, the shape of the output voltage pulse depends on the energy of the incident photon. For example, one could integrate the output voltage pulse of SSPD 12 as a function of time and find a correlation between the incident photon energy and the integral of the pulse.

FIG. 7 shows traces captured by oscilloscope 71 (FIG. 4A) in one experiment. Trace 701 shows the output signal of photodetector 64 upon detection of light pulses received from beam splitter 62. Trace 702 shows the amplified output signal of SSPD 12 for incident light pulse powers corresponding to an average of 100 incident photons per device area, per light pulse. In that case, the probability of SSPD 12 producing an output voltage pulse for each incident light pulse is 100%. Trace 703 shows the amplified output signal of SSPD 12 for incident light pulse powers corresponding to an average of 40 photons per device area, per light pulse. Similarly, traces 704, 705, 706, 707, and 708 show the amplified output signal of SSPD 12 for incident pulse powers corresponding to an average of 10, 5, 5, 1, and 1 photon per device area, per light pulse, respectively. Traces 707 and 708 demonstrate that SSPD 12 has enough sensitivity to

detect a single photon. The traces also show that the detected pulse has approximately the same shape and amplitude regardless of how many photons are absorbed.

5           FIGS. 8A-8C show diagrams of various arrangements for coupling light to the SSPD. Note that FIGS. 8A-8C are schematic representations and not drawn to scale (for example, SSPD 12 in actuality has practically zero thickness relative to its substrate). In FIG. 8A,  
10 incident light beam 16 passes through an aperture diaphragm 802 in front of a hemispherical lens 803. Substrate 823 of SSPD 12 functions as an optical extension and is directly bonded to hemispherical lens 803. Light beam 16 is focused onto SSPD 12 through  
15 hemispherical lens 803 and substrate 823. Hemispherical lens 803 and substrate 823 are preferably of the same material so that the diameter of aperture diaphragm 802 can be maximized. SSPD 12 can also be mounted with its superconducting film directly facing  
20 light beam 16 (on the other end of substrate 823) by extending hemispherical lens 803. In FIG. 8B, SSPD 12 receives the incident light beam from a single-mode or multi-mode fiber 805. Light that is not absorbed by SSPD 12 passes through substrate 823 and into mirror  
25 806 where the light is reflected off a mirrored surface 807 and focused onto SSPD 12. In FIG. 8C, incident free-propagating light beam 16 passes through anti-reflective coating 808, substrate 823, and quartz (or silicon for infrared applications) parabolic lens 810.  
30 Light beam 16 is reflected off mirrored surface 811 and focused onto SSPD 12.

While specific embodiments of this invention have been described, it is to be understood that these  
35 embodiments are illustrative and not limiting. Many additional embodiments that are within the broad

principles of this invention will be apparent to  
persons skilled in the art.

CLAIMS

What is claimed is:

- 5           1.    A method of detecting photons, comprising the  
acts of:
- providing a superconductor strip;  
              electrically biasing said superconductor  
              strip; and  
10           directing light onto said biased  
superconductor strip;  
              wherein said biasing is at a level near said  
superconductor strip's critical current thereby to  
detect a single photon incident on said  
15           superconductor strip.
2.    The method of claim 1 wherein said single  
photon is detected by measuring an output pulse from  
said superconductor strip.
- 20           3.    The method of claim 1 wherein said  
superconductor strip is of niobium nitride.
4.    The method of claim 1 wherein said single  
25           photon has a wavelength between the visible and the far  
infrared spectral regions.
5.    The method of claim 1 wherein said  
superconductor strip defines a meander.
- 30           6.    The method of claim 2 wherein said  
superconductor strip has a width equal to or less than  
about 200nm.
- 35           7.    A photon detector comprising a  
superconducting film coupled to a bias source, wherein

said superconducting film is biased near its critical current, and wherein said superconducting film has a dimension which allows detection of a single incident photon.

5

8. The photon detector of claim 7 wherein said superconducting film is of niobium nitride.

9. The photon detector of claim 7 wherein a  
10 width of said superconducting film is equal to or less than about 200nm.

10. The photon detector of claim 7 wherein said superconducting film forms a detectable resistive  
15 region upon absorption of said single incident photon.

11. The photon detector of claim 7 further comprising:  
a plurality of contact pads coupled to ends  
20 of said superconducting film; and  
wherein said bias source is coupled to said superconducting film at said plurality of contact pads.

12. The photon detector of claim 7 wherein said superconducting film defines a meander.

13. The photon detector of claim 11 wherein said contact pads include gold.

30

14. The photon detector of claim 7 wherein light is coupled to said superconducting film using an optical fiber.



15. The photon detector of claim 7 wherein light is coupled to said superconducting film through a hemispherical lens.

## SUPERCONDUCTING SINGLE PHOTON DETECTOR

Roman Sobolewski  
Grigory N. Gol'tsman  
Alexey D. Semenov  
Oleg V. Okunev  
Kenneth R. Wilsher  
Steven A. Kasapi

### ABSTRACT OF THE DISCLOSURE

A single-photon detector includes a superconductor strip biased near its critical current. The superconductor strip provides a discernible output signal upon absorption of a single incident photon. In one example, the superconductor is a strip of NbN (niobium nitride). In another example, the superconductor strip meanders to increase its probability of receiving a photon from a light source. The single-photon detector is suitable for a variety of applications including free-space and satellite communications, quantum communications, quantum cryptography, weak luminescence, and semiconductor device testing.

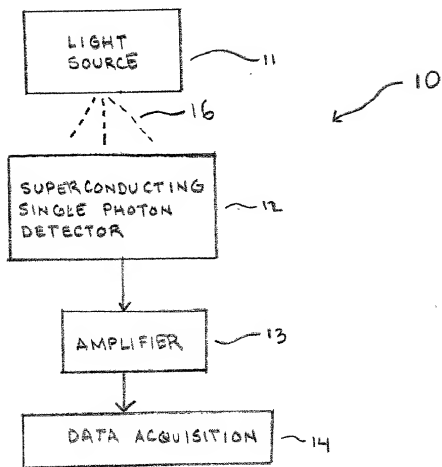
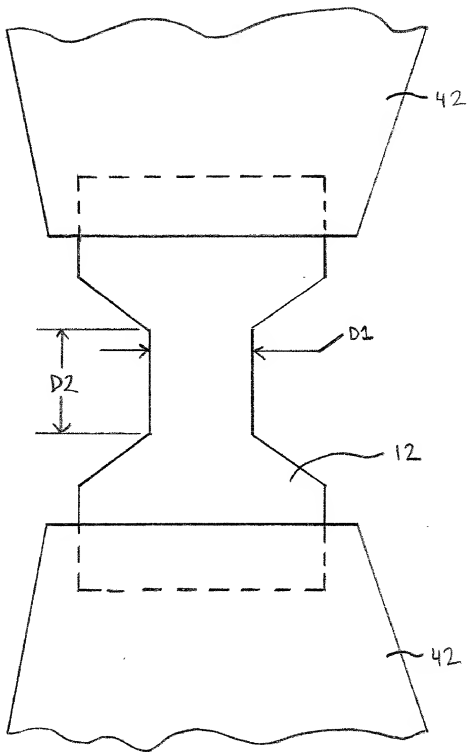


FIG. 1A

Country	Year	Population (millions)	Urban population (millions)	Urban population (%)	Population density (per sq km)	Urban population density (per sq km)
Algeria	1980	10.0	4.0	40.0	100	400
Algeria	1985	10.5	4.5	42.9	105	429
Algeria	1990	11.0	5.0	45.5	110	455
Algeria	1995	11.5	5.5	47.8	115	478
Algeria	2000	12.0	6.0	50.0	120	500
Algeria	2005	12.5	6.5	52.0	125	520
Algeria	2010	13.0	7.0	53.8	130	538
Algeria	2015	13.5	7.5	55.6	135	556
Algeria	2020	14.0	8.0	57.1	140	571
Algeria	2025	14.5	8.5	58.6	145	586
Algeria	2030	15.0	9.0	60.0	150	600
Algeria	2035	15.5	9.5	61.3	155	613
Algeria	2040	16.0	10.0	62.5	160	625
Algeria	2045	16.5	10.5	63.6	165	636
Algeria	2050	17.0	11.0	64.7	170	647
Algeria	2055	17.5	11.5	65.7	175	657
Algeria	2060	18.0	12.0	66.7	180	667
Algeria	2065	18.5	12.5	67.6	185	676
Algeria	2070	19.0	13.0	68.4	190	684
Algeria	2075	19.5	13.5	69.2	195	692
Algeria	2080	20.0	14.0	70.0	200	700
Algeria	2085	20.5	14.5	70.7	205	707
Algeria	2090	21.0	15.0	71.4	210	714
Algeria	2095	21.5	15.5	72.1	215	721
Algeria	2100	22.0	16.0	72.7	220	727
Algeria	2105	22.5	16.5	73.3	225	733
Algeria	2110	23.0	17.0	73.9	230	739
Algeria	2115	23.5	17.5	74.5	235	745
Algeria	2120	24.0	18.0	75.0	240	750
Algeria	2125	24.5	18.5	75.5	245	755
Algeria	2130	25.0	19.0	76.0	250	760
Algeria	2135	25.5	19.5	76.5	255	765
Algeria	2140	26.0	20.0	76.9	260	769
Algeria	2145	26.5	20.5	77.3	265	773
Algeria	2150	27.0	21.0	77.8	270	778
Algeria	2155	27.5	21.5	78.2	275	782
Algeria	2160	28.0	22.0	78.6	280	786
Algeria	2165	28.5	22.5	78.9	285	789
Algeria	2170	29.0	23.0	79.3	290	793
Algeria	2175	29.5	23.5	79.7	295	797
Algeria	2180	30.0	24.0	80.0	300	800
Algeria	2185	30.5	24.5	80.3	305	803
Algeria	2190	31.0	25.0	80.6	310	806
Algeria	2195	31.5	25.5	81.0	315	810
Algeria	2200	32.0	26.0	81.3	320	813
Algeria	2205	32.5	26.5	81.6	325	816
Algeria	2210	33.0	27.0	81.8	330	818
Algeria	2215	33.5	27.5	82.1	335	821
Algeria	2220	34.0	28.0	82.4	340	824
Algeria	2225	34.5	28.5	82.6	345	826
Algeria	2230	35.0	29.0	82.9	350	829
Algeria	2235	35.5	29.5	83.1	355	831
Algeria	2240	36.0	30.0	83.3	360	833
Algeria	2245	36.5	30.5	83.6	365	836
Algeria	2250					



NOTE:  
NOT TO SCALE

FIG. 1B

1. The first group of people who are not in the majority are those who are not in the majority.

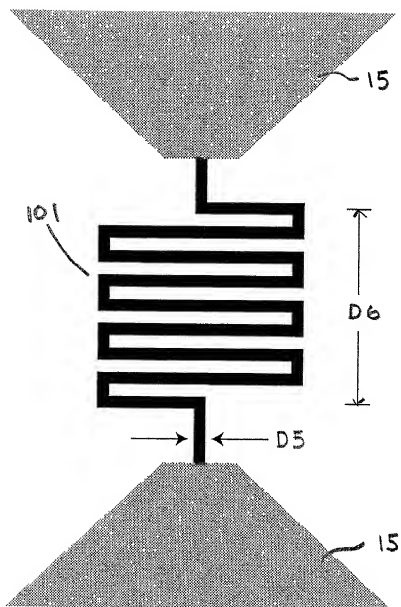


FIG. 1C

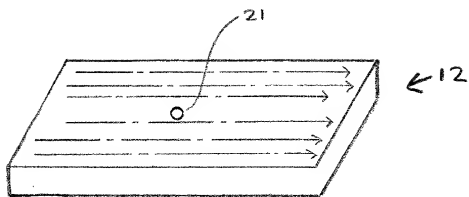


FIG. 2A

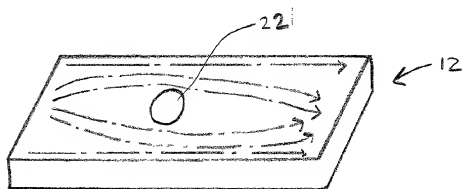


FIG. 2B

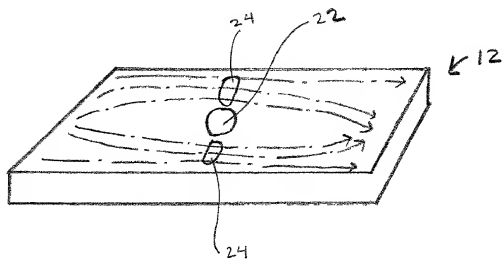


FIG. 2C

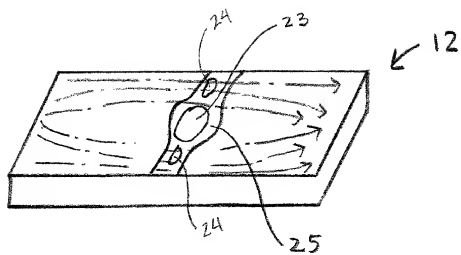


FIG. 2D

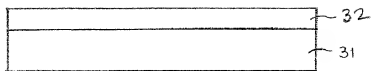


FIG. 3A

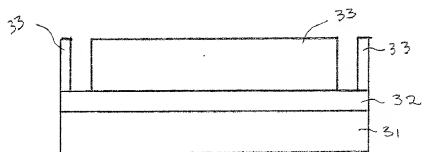


FIG. 3B

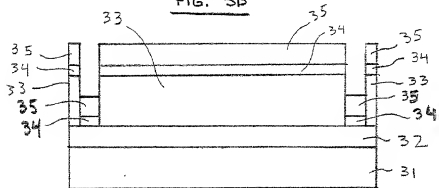


FIG. 3C

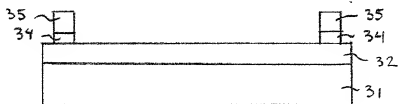


FIG. 3D



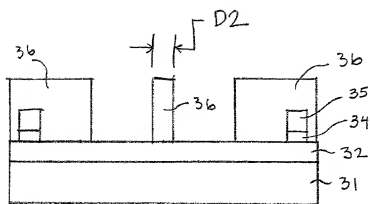


FIG. 3E

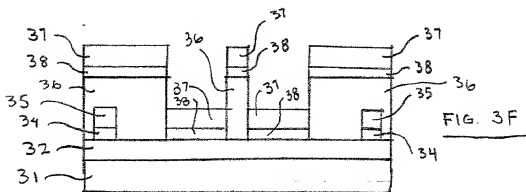


FIG. 3F

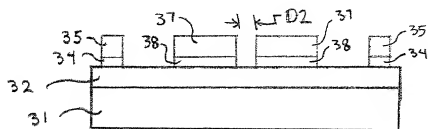


FIG. 3G

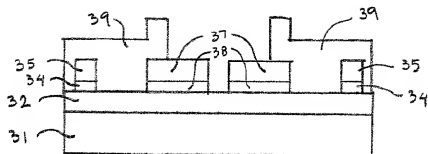


FIG. 3H

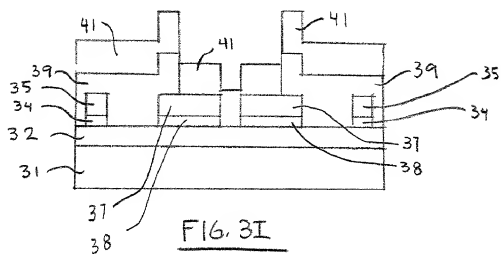


FIG. 3I

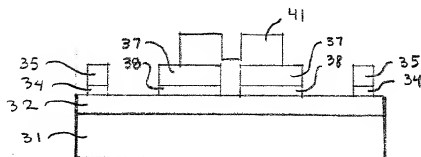


FIG. 3J



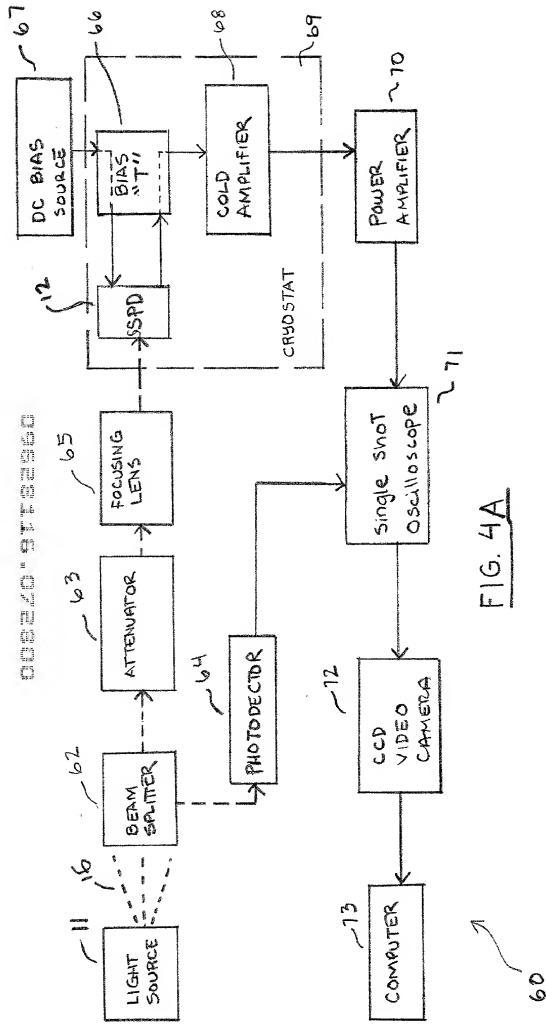


FIG. 4A

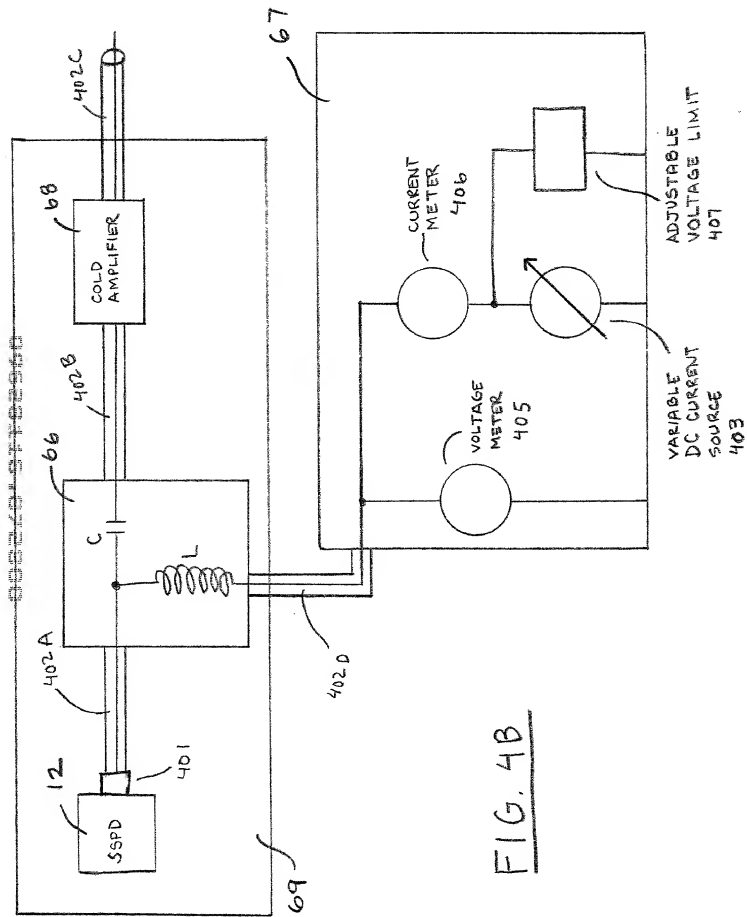


FIG. 4B

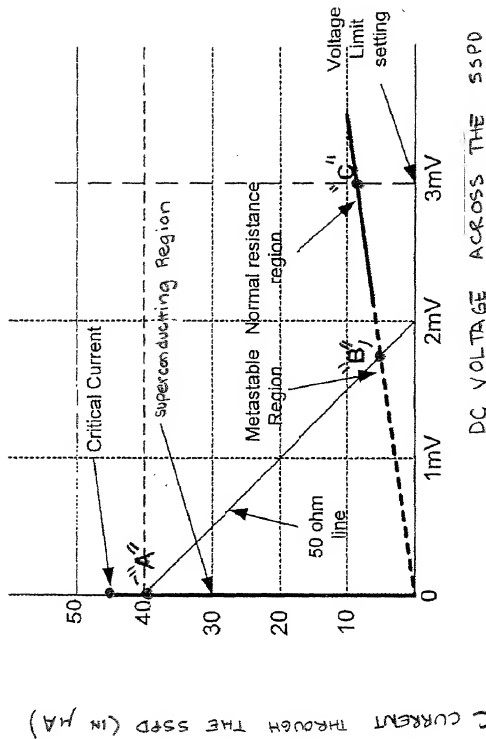


FIG. 4C

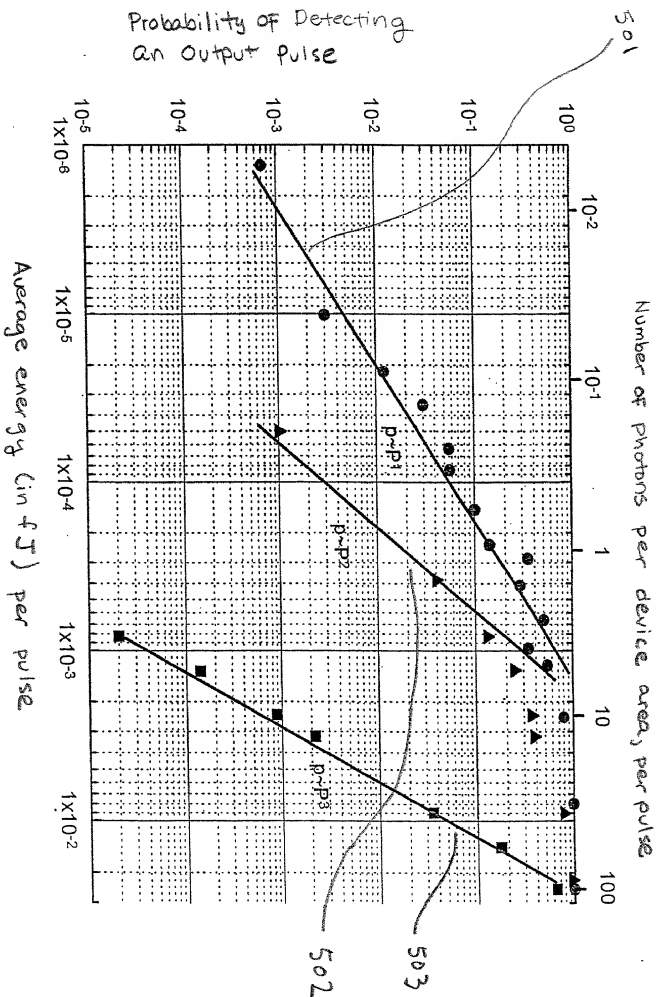


FIG. 5

09628116-072800

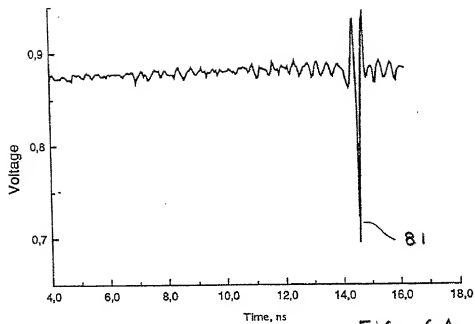


FIG. 6A

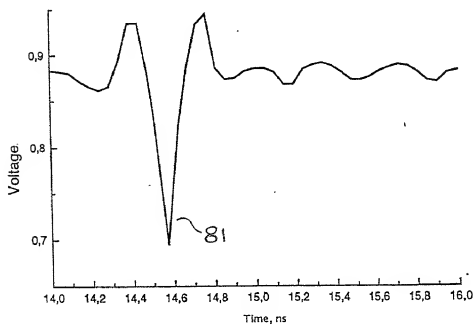


FIG. 6B



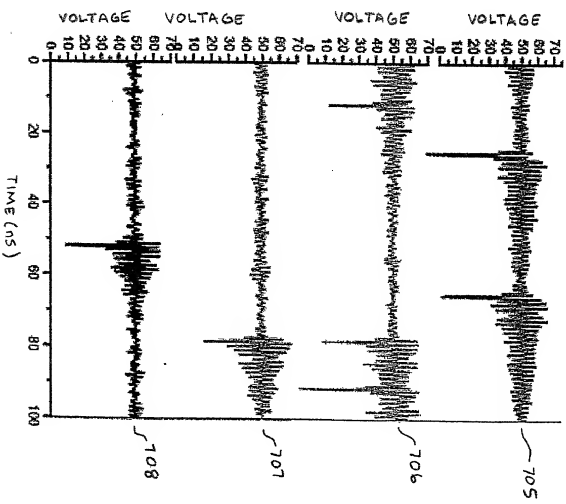
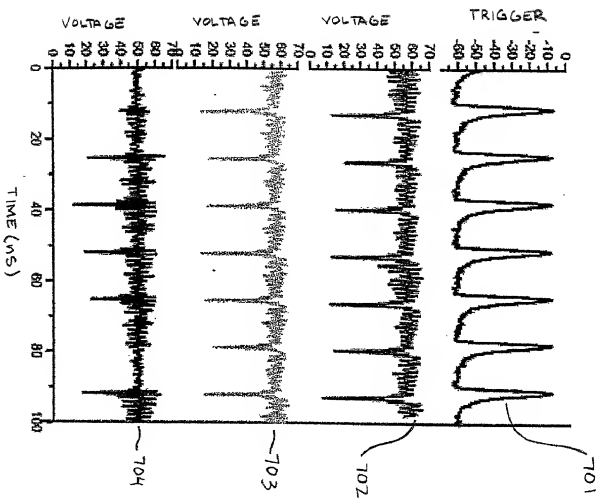


FIG. 7

0962016.072800

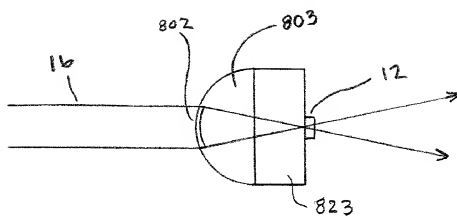


FIG. 8A

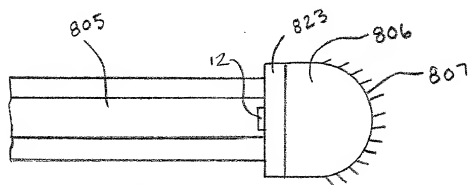


FIG. 8B

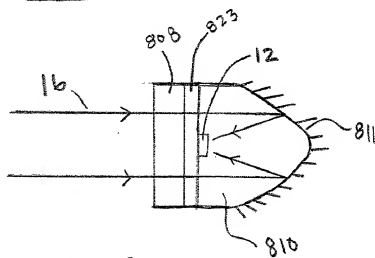


FIG. 8C

# DECLARATION FOR PATENT APPLICATION AND POWER OF ATTORNEY

As a below named inventor, I hereby declare that:

My residence, post office address and citizenship are as stated below adjacent to my name.

I believe I am an original, first and joint inventor of subject matter (process, machine, manufacture, or composition of matter, or an improvement thereof) which is claimed and for which a patent is sought by way of the application entitled

## Superconducting Single Photon Detector

which (check) ☒ is attached hereto.  
☐ and is amended by the Preliminary Amendment attached hereto.  
☐ was filed on \_\_\_\_\_ as Application Serial No.  
☐ and was amended on \_\_\_\_ (if applicable).

I hereby state that I have reviewed and understand the contents of the above identified specification, including the claims, as amended by any amendment referred to above.

I acknowledge the duty to disclose information, which is material to patentability as defined in Title 37, Code of Federal Regulations, § 1.56.

I hereby claim foreign priority benefits under Title 35, United States Code, § 119(a)-(d) of any foreign application(s) for patent or inventor's certificate or any PCT international application(s) designating at least one country other than the United States of America listed below and have also identified below any foreign application(s) for patent or inventor's certificate or any PCT international application(s) designating at least one country other than the United States of America filed by me on the same subject matter having a filing date before that of the application(s) of which priority is claimed:

Prior Foreign Application(s)			Priority Claimed	
Number	Country	Day/Month/Year Filed	Yes	No
N/A			<input type="checkbox"/>	<input type="checkbox"/>

I hereby claim the benefit under Title 35, United States Code, § 119(e) of any United States provisional application(s) listed below:

Provisional Application Number	Filing Date
N/A	

I hereby claim the benefit under Title 35, United States Code, § 120 of any United States application(s) or PCT international application(s) designating the United States of America listed below and, insofar as the subject matter of each of the claims of this application is not disclosed in the prior application(s) in the manner provided by the first paragraph of Title 35, United States Code, § 112, I acknowledge the duty to disclose information, which is material to patentability as defined in Title 37, Code of Federal Regulations, § 1.56, which became available between the filing date of the prior application(s) and the national or PCT international filing date of this application:

Application Serial No.	Filing Date	Status (patented, pending, abandoned)
N/A		

I hereby appoint the following attorney(s) and/or agent(s) to prosecute this application and to transact all business in the United States Patent and Trademark Office connected therewith:

Alan H. MacPherson (24,423); Brian D. Ogonowsky (31,988); David W. Heid (25,875); Norman R. Klivans (33,003); Edward C. Kwok (33,938); David E. Steuber (25,557); Michael Shenker (34,250); Stephen A. Terrile (32,946); Peter H. Kang (40,350); Ronald J. Meetin (29,089); Ken John Koestner (33,004); Omkar K. Suryadevara (36,320); David T. Millers (37,396); Michael P. Adams (34,763); Robert B. Morrill (43,817); James E. Parsons (34,691); Philip W. Woo (39,880); Emily Haliday (38,903); Tom Hunter (38,498); Michael J. Halbert (40,633); Gary J. Edwards (41,008); Daniel P. Stewart (41,332); John T. Winburn (26,822); Tom Chen (42,406); Fabio E. Marino (43,339); Don C. Lawrence (31,975); Marc R. Ascolese (42,268); Carmen C. Cook (42,433); David G. Dolezal (41,711); Roberta P. Saxon (43,087); Mary Jo Bertani (42,321); Dale R. Cook (42,434); Sam G. Campbell (42,381); Matthew J. Brigham (44,047); Hugh H. Matsubayashi (43,779); Patrick D. Benedicto (40,909); T.J. Singh (39,535); Shireen Irani Bacon (40,494); Rory G. Bens (44,028); George Wolken, Jr. (30,441); John A. Odozynski (28,769); Cameron K. Kerrigan (44,826); Paul E. Lewkowicz (44,870); Theodore P. Lopez (44,881); Mayankkumar M. Dixit (44,064); Eric Stephenson (38,321); Christopher Allenby (45,906); David C. Hsia (46,235); Mark J. Rozman (42,117); Margaret M. Kelton (44,182); Do Te Kim (46,231); Alex Chen (45,591); Monique M. Heyninck (44,763); Gregory J. Michelson (44,940); Jonathan Geld (44,702); Emmanuel Rivera (45,760); Jason Farhadian (42,523); Matthew J. Spark (43,453); and Elaine H. Lo (41,158).

Please address all correspondence and telephone calls to:

Norman R. Klivans  
Attorney for Applicants  
**SKJERVEN MORRILL MacPHERSON LLP**  
25 Metro Drive, Suite 700  
San Jose, California 95110-1349

Telephone: 408-453-9200  
Facsimile: 408-453-7979

I declare that all statements made herein of my own knowledge are true, all statements made herein on information and belief are believed to be true, and all statements made herein are made with the knowledge that whoever, in any matter within the jurisdiction of the Patent and Trademark Office, knowingly and willfully falsifies, conceals, or covers up by any trick, scheme, or device a material fact, or makes any false, fictitious or fraudulent statements or representations, or makes or uses any false writing or document knowing the same to contain any false, fictitious or fraudulent statement or entry, shall be subject to the penalties including fine or imprisonment or both as set forth under 18 U.S.C. 1001, and that violations of this paragraph may jeopardize the validity of the application or this document, or the validity or enforceability of any patent, trademark registration, or certificate resulting therefrom.

Full name of first joint inventor:	Roman Sobolewski		
Inventor's Signature:		Date:	
Residence:	Pittsford, New York 14534		
Post Office Address:	3 Cambric Circle	Citizenship:	POLAND
	Pittsford, NY 14534		

Full name of second joint inventor:	Grigory N. Gol'tsman		
Inventor's Signature:		Date:	
Residence:	Moscow, Russia		
Post Office Address:	74 Altufevskoe Ch., Apt. 501	Citizenship:	RUSSIA
	Moscow, 127349, Russia		

Full name of third joint inventor:	Alexey D. Semenov		
Inventor's Signature:		Date:	
Residence:	Moscow, Russia		
Post Office Address:	11 Lukinskaya Street, Apt. 616	Citizenship:	RUSSIA
	Moscow, 119634, Russia		

Full name of fourth joint inventor:	Oleg V. Okunev		
Inventor's Signature:		Date:	
Residence:	Moscow, Russia		
Post Office Address:	4 Ak. Vinogradova Street, Apt. 172	Citizenship:	RUSSIA
	Moscow, 113143, Russia		

Full name of fifth joint inventor:	Kenneth R. Wilsher		
Inventor's Signature:		Date:	
Residence:	Palo Alto, California		
Post Office Address:	1085 Emerson St	Citizenship:	USA
	Palo Alto, CA 94301		

Full name of sixth joint inventor:	Steven A. Kasapi		
Inventor's Signature:		Date:	
Residence:	San Francisco, California		
Post Office Address:	584 Castro Street	Citizenship:	CANADA
	San Francisco, CA 94114		